ISTITUTO
DI
ANALISI NUMERICA

del

CONSIGLIO NAZIONALE DELLE RICERCHE
via Ferrata 1 – 27100 PAVIA (Italy)

PAVIA
2002

PUBBLICAZIONI

N. 1311

Enrico Bertolazzi, Gianmarco Manzini

A unified treament of boundary conditions in least square-based Finite Volume methods

A unified treament of boundary conditions in least square-based Finite Volume methods

Enrico Bertolazzi [a] Gianmarco Manzini [b]

[a] *Dip. Ingegneria Meccanica e Strutturale,*
Università di Trento,
via Mesiano 77, Trento, Italy

[b] *Istituto di Analisi Numerica - CNR,*
via Ferrata 1, 27100 Pavia, Italy

Abstract

We propose a unified treatment of internal and boundary vertex Least Squares reconstructions in second-order accurate cell-centered finite volume discretisation of 2-D steady diffusion problems. Dirichlet, Neumann and Robin boundary conditions are taken into account in the same formulation by introducing suitable constraints in the Least Squares minimization process. The method is discussed in its theoretical framework and a representative numerical experiment illustrates its capability in providing the second order of accuracy.

Key words: Finite Volume, Unstructured mesh, Neumann Boundary Conditions, Robin Boundary Conditions, Least Squares reconstruction.

1 Introduction

Let us consider the second-order steady diffusion problem

$$\begin{aligned} \operatorname{div}(\nu\nabla u) &= f \quad \text{on } \Omega, \\ \alpha u + \beta\mathbf{n}\cdot\nu\nabla u &= g \quad \text{on } \partial\Omega, \end{aligned} \tag{1}$$

for the unknown scalar field u on the domain $\Omega \subset \mathbb{R}^2$ with closed boundary $\partial\Omega$. In equations (1), ν is the scalar viscosity field and f a forcing term. In (1), $\mathbf{n}$ is the outward-directed normal vector to $\partial\Omega$, g is a suitable boundary function which yields the boundary conditions on $\partial\Omega$ and α and β two switch coefficients. This formulation of the boundary conditions is quite general, because it allows us to take into account simultaneously the following cases:

(i) *Dirichlet* boundary conditions, $\alpha = 1$, $\beta = 0$;
(ii) *Neumann* boundary conditions, $\alpha = 0$, $\beta = 1$;
(iii) *Robin* boundary conditions, $\alpha = 1$, $\beta = 1$.

Boundary conditions of mixed type are also included. The domain boundary $\partial\Omega$ can indeed be split into the union of distinct connected subsets where different choices of α and β are set. We outline that mixed boundary conditions are required when the Neumann condition (ii) is taken into account. Otherwise, case (ii) alone would certainly lead to a singular discretization [1]. Under suitable assumptions on the regularity of the closed boundary contour $\partial\Omega$ and the boundary function g, problem (1) can be re-formulated in a weak form, and the existence and uniqueness of the analytical solution can be proved [2].

In this work we consider the 2-nd order accurate finite volume discretization that is generally referred to as *diamond scheme* in literature. As usual in Finite Volumes, a linear operator is built by re-formulating in a discrete way the element-wise flux balance integrals. A numerical diffusive flux function is introduced at this stage, which makes usage of cell-average solution values and an estimate of the vertex solution values. These latters are obtained from the cell-average ones by applying a special averaging procedure that ensures formal second order of accuracy. Let us indicate by u_k the cell-average value of the cell T_k, and by u_{v} the reconstructed solution at the boundary vertex v of coordinates $\mathbf{x}_{\mathsf{v}}$.

Formally, we can write

$$u_{\mathsf{v}} = \sum_{k \in \sigma_{\mathsf{v}}} \omega_k^{\mathsf{v}} u_k, \tag{2}$$

where the summation index k runs throughout the set σ_{v} of the cells adjacent v and the cell averages u_k are multiplied by suitable weight factors ω_k^{v}. The reconstruction weights can be determined in several ways that are widely applied in Computational Fluid Dynamics applications and well documented in literature. To this purpose, it is certainly worth mentioning the weights provided by the simple arithmetic average technique [3,4], by the cell area ratio technique [5], by the inverse distance ratio technique [6–9], and by the Least Squares approximation process [10].

It turns out that special care must be deserved to the treatment of the boundary conditions in this reconstruction step. The treatment of a Dirichlet boundary vertex is rather simple and consists in imposing directly the boundary value. Thus, we set $u_{\mathsf{v}} = g(\mathbf{x}_{\mathsf{v}})$ in place of (2). The situation is much more complex for a vertex showing a Neumann or a Robin condition. In these two latter cases, the point-wise values are usually estimated by the *ghost cell technique* [1]. Basically, this technique applies the same reconstruction procedure of an internal vertex to an extended set of cell-averaged data which includes *ghost cell* data defined on *ghost cells*. The ghost cells are images of the boundary cells incident v and built by specular reflections across the boundary and the internal edges. Ghost cell data are estimated by an extrapolation process, usually based on a 1-st order Taylor series development [1]. The vertex value reconstructed by this method reads as

$$u_{\mathsf{V}} = \sum_{k \in \sigma_{\mathsf{V}}} \omega_k^{\mathsf{V}} u_k + \sum_{k' \in \sigma'_{\mathsf{V}}} \omega_{k'}^{\mathsf{V}} u_{k'}.$$

The first summation index, k, runs throughout the set of "real" cells σ_{V}, while the second one, k', runs throughout the set σ'_{V} of ghost cells. This latter summation term takes into account fictitious ghost cell data $u_{k'}$ multiplied by the ghost cell weight factors $\omega_{k'}^{\mathsf{V}}$.

As documented in literature, this treatment of the boundary conditions have shown in more complex fluid dynamics applications "suspect" behaviors that deserve further investigation [7–9].

In this paper, we propose a different approach that generalises to the boundary vertex case the internal vertex reconstruction procedure by introducing the boundary conditions as constraints in the vertex Least Squares reconstruction process. Our method allows a unique definition for Dirichlet, Neumann and Robin conditions, and preserves the required 2-nd order of accuracy of the finite volume discretization. Furthermore, our technique does not require any modification of the discrete finite volume operator to include the boundary condition treatment. This method can thus be easily incorporated with minimum effort into pre-existent software implementations.

The outline of the paper follows. In Section 2 we present a short review of the finite volume method that forms the framework of the vertex Least square reconstruction algorithm. This latter one is presented and discussed in full details in Section 3. Then, in Section 4 we illustrate the performance of this method on a representative test case. Finally, in Section 5 we draw the conclusions.

2 The 2-nd order Finite Volume formulation

Let us shortly review for exposition's sake the 2-nd order accurate cell-centered Finite Volumes into which the Least Squares vertex reconstruction is naturally incorporated. This section is mainly based on References [3,11].

As usual in cell-centered finite volume approximations, we assume that the computational domain Ω be covered by an unstructured mesh $\mathcal{T}_h$. The mesh $\mathcal{T}_h$ is a collection of N_{T} non-empty and non-overlapping control volumes, namely

T_i, which are two-dimensional simplices (triangles). The mesh size h is defined as the supremum of the mesh control volume diameters [12]. The set $\Omega_h = \cup_{i=1}^{N_\mathsf{T}} \mathsf{T}_i \subseteq \Omega$ is a polygonal approximation of Ω.

Convergence analysis introduces a set of constraints on the sequence of meshes as the size factor h tends to zero, leading to the concept of *finite volume admissible meshes* in accord with the definition given in References [3,11]. We strenghten these conditions by requiring that the admissible meshes furtherly satisfy:

- *Assumption 1*, there exists a real positive constant γ independent of h that bounds every mesh angles from below;
- *Assumption 2*, there exist at least three cells incident every mesh boundary vertex, whose centroids are non collinear.

Assumption 1 introduces a *minimum angle condition* that avoids too stretched or skewed meshes in the convergence process $h \rightarrow 0$. It is similar to the angle condition usually taken into account in finite element discretisation [12]. Assumption 2 clearly implies that a boundary vertex must be shared by at least three control volumes. We will demonstrate in the next section that Assumption 2 ensures the well posedness of the linear algebraic problem resulting from the proposed scheme because a linear two-dimensional approximation requires the specification of three independent degrees of freedom. We will also show that Assumption 2 can be partially relaxed, at the price of introducing a problem dependent constraint on the finite volume meshes.

The cell-centered finite volume method on $\mathcal{T}_h$ is derived as usual by integrating equation (1) on T_i and then applying the Gauss-Green divergence theorem [11]. This yields the flux balance integral equation

$$\int\limits_{\partial \mathsf{T}_i} \mathbf{n} \cdot \nu \nabla u \, dl = \int\limits_{\mathsf{T}_i} f \, d\mathbf{x}, \qquad \text{for } i = 1, \ldots N_\mathsf{T}, \tag{3}$$

defined on the boundary $\partial \mathsf{T}_i$ of the i-th control volume T_i.

Let us indicate by $\mathbf{u}$ the solution vector, whose i-th component u_i is the finite volume approximation of the i-th cell-averaged solution. The finite volume method mimicks (3) by substituting the integrals of the diffusive flux $\mathbf{n} \cdot \nu \nabla u$ across the edge $\mathsf{e}_{ij} \subset \partial \mathsf{T}_i$ by its discrete counterpart denoted by $\mathsf{G}_{ij}(\mathbf{u})$. The righ-hand-side source integral is calculated by a quadrature formula of the correct order of accuracy and indicated by f_i. This approach leads to state the set of equations

$$\sum_{j \in \sigma_i} \mathsf{G}_{ij}(\mathbf{u}) = f_i, \qquad \text{for } i = 1, \ldots N_\mathsf{T}, \tag{4}$$

that correlates the cell-average approximations and ghost-cell values u_i labeled by the index set σ_i of the cells adjacent to T_i and boundary edges in $\partial\mathsf{T}_i \cap \partial\Omega$.

The numerical diffusive flux integral is defined by

$$\mathsf{G}_{ij}(\mathbf{u}) = -\left|\mathsf{e}_{ij}\right| \nu_{ij}\mathbf{n}_{ij} \cdot \mathcal{G}^{\diamond}_{ij}(\mathbf{u}), \tag{5}$$

where $\nu_{ij} = \int_{\mathsf{e}_{ij}} \nu(\mathbf{x})\, d\mathbf{x}$, and $\mathcal{G}^{\diamond}_{ij}(\mathbf{u})$ is the numerical estimate of the solution gradient provided at the edge e_{ij} of lenght $|\mathsf{e}_{ij}|$ by the *diamond scheme* [3]. Since $\mathcal{G}^{\diamond}_{ij}(\mathbf{u})$ is a linearly dependent function of its argument $\mathbf{u}$, substituting equation (5) in equation (4) yields a linear algebraic problem whose solution is indeed the cell-average vector $\mathbf{u}$.

The normal component of the numerical gradient $\mathcal{G}^{\diamond}_{ij}(\mathbf{u})$ in (5) is defined throughout the following steps. First, we introduce a *one-side edge-centered* approximation of the normal derivative $\mathbf{n} \cdot \nabla u$, namely $\mathbf{n}_{ij} \cdot \mathcal{G}_{ij}$. Then, we distinguish the case of an internal and a boundary edge. At an internal edge, a conservative definition is achieved by averaging the two one-side numerical gradients $\mathcal{G}_{ij}(\mathbf{u})$ and $\mathcal{G}_{ji}(\mathbf{u})$, respectively defined within the control volumes T_i and T_j adjacent the edge e_{ij}. The average gradient is

$$\mathcal{G}^{\diamond}_{ij}(\mathbf{u}) = W_{ij}\mathcal{G}_{ij}(\mathbf{u}) + W_{ji}\mathcal{G}_{ji}(\mathbf{u}).$$

The weights yielding the diamond scheme are

$$W_{ij} = \frac{|\mathsf{T}_i|}{|\mathsf{T}_i| + |\mathsf{T}_j|}, \qquad \text{and} \qquad W_{ji} = \frac{|\mathsf{T}_j|}{|\mathsf{T}_i| + |\mathsf{T}_j|}.$$

At a boundary edge, the conservative discrete gradient is given by taking the unique available edge gradient, that is $\mathcal{G}^{\diamond}_{ij}(\mathbf{u}) = \mathcal{G}_{ij}(\mathbf{u})$.

The *one-side edge-centered* approximation of the normal component of the solution gradient, that is $\mathbf{n}_{ij} \cdot \mathcal{G}_{ij}(\mathbf{u})$, is estimated by applying the Gauss-Green theorem to the simplex whose vertices are the centroid of T_i and the vertices of the edge e_{ij}. Let us denote by $\tilde{\mathbf{x}}_{ij} \in \mathsf{e}_{ij}$ the orthogonal projection of the centroid of T_i onto the edge e_{ij}. After some algebraic manipulations, the one-side edge-centered gradient can be re-written as

$$\mathbf{n}_{ij} \cdot \mathcal{G}_{ij}(\mathbf{u}) = \frac{\tilde{u}_{ij} - u_i}{h_{ij}},$$

where h_{ij} is the distance between $\tilde{\mathbf{x}}_{ij}$ and $\mathbf{x}_i$, and

$$\tilde{u}_{ij} = \sum_{\mathsf{V} \in \mathcal{V}_i \cap \mathcal{V}_j} \lambda^{ij}_{\mathsf{V}} u_{\mathsf{V}}$$

is the linearly interpolated value of $u|_{\mathsf{T}_i}$ at $\tilde{\mathbf{x}}_{ij}$. This latter term is expressed by using the vertex values u_{V} and the linearly interpolating coefficients at $\tilde{\mathbf{x}}_{ij}$, namely $\lambda^{ij}_{\mathsf{V}}$, with respect to v for any $\mathsf{v} \in \mathcal{V}_j \cap \mathcal{V}_j$. From Assumption 1 it follows that $\tilde{\mathbf{x}}_{ij}$ is an interior point of the edge e_{ij}, and, consequently, that the linearly interpolating coefficients are strictly positive. In this case, u_{ij} is a *convex* linear combination of the vertex values u_{V}.

Finally, let us outline that in order to achieve a second-order accurate discretization, the diamond scheme requires that at any mesh edge e_{ij} the numerical gradients $\mathcal{G}_{ij}$ of the numerical diffusive flux be estimated to at least $\mathcal{O}(h)$ order of accuracy. This is given by using the linear Least Squares reconstruction algorithm described in the next section to approximate the cell-vertex values from the cell-averaged finite volume approximations.

3 Least Squares vertex reconstruction

A linear approximation of the analytical solution is built from the cell-averaged data set

$$\{(\mathbf{x}_k,\, u_k),\, k \in \sigma_{\mathsf{V}}\}$$

within the macro-element $\cup_{k\in\sigma_{\mathsf{V}}}\mathsf{T}_k$ by applying the Least Squares Method. This approximation takes the form

$$u_{\mathsf{V}}(\mathbf{x}) = a + \mathbf{b}\cdot(\mathbf{x}-\mathbf{x}_{\mathsf{V}}), \qquad \mathbf{x}\in\cup_{k\in\sigma_{\mathsf{V}}}\mathsf{T}_k, \tag{6}$$

in terms of the vector of coefficients a and $\mathbf{b}$. For the sake of notation compactness, we will also use throughout this section the LS coefficient vector $\mathfrak{z}^T = (a,\, \mathbf{b}^T)$. The following proposition is the basic result of this paper.

Proposition 1 *The reconstructed value $u_{\mathsf{V}} = u_{\mathsf{V}}(\mathbf{x}_{\mathsf{V}})$ of the vertex v – no matter this one is an internal or a boundary vertex – takes the form of the affine linear combination of the surrounding cell-averaged values,*

$$u_{\mathsf{V}} = \sum_{k\in\sigma_{\mathsf{V}}} \omega_k^{\mathsf{V}} u_k + \tilde{u}_{\mathsf{V}}, \tag{7}$$

where $\{\omega_k^{\mathsf{V}},\, k\in\sigma_{\mathsf{V}}\}$ are the weights and $\tilde{u}_{\mathsf{V}}$ a special displacement value produced by the Least Squares process.

Essentially, we claim in proposition 1 that the Least Squares interpolation technique, which has been proposed in literature just for the reconstruction of the values at internal vertices, can be suitably generalized to take into account both internal and boundary vertices.

In the rest of this section we prove this result discussing separately the case of an internal and a boundary vertex. In both cases we derive a formula to compute efficiently the weights and the displacements generated by the Least Squares method.

The linear Least Squares approximation is given by taking the coefficient vector $(a,\,\mathbf{b})^T$ as the minimizer of the functional

$$\mathcal{J}\,(a,\,\mathbf{b}) = \sum_{k\in\sigma_{\mathsf{V}}} \lambda_k \left[a + \mathbf{b}\cdot(\mathbf{x}_k - \mathbf{x}_{\mathsf{V}}) - u_k\right]^2,$$

where $\{\lambda_k\}$ is a suitable set of strictly positive weights normalized to a unit sum. Usual choices are $\lambda_k = \frac{1}{N_{\mathsf{V}}}$ [3,4], where N_{V} is the cardinality of the set σ_{V} of the triangles incident to v, $\lambda_k = \frac{\left|\mathbf{x}_k - \mathbf{x}_{\mathsf{V}}\right|^{-1}}{\sum_{k\in\sigma_{\mathsf{V}}}\left|\mathbf{x}_k - \mathbf{x}_{\mathsf{V}}\right|^{-1}}$ [6–9], $\lambda_k = \frac{|\mathsf{T}_k|}{\sum_{k\in\sigma_{\mathsf{V}}}|\mathsf{T}_k|}$ [5].

Imposing the null gradient condition

$$\nabla_{\mathfrak{Z}}\mathcal{J}(\mathfrak{Z}) = \mathbf{0}$$

leads to the algebraic system usually known as *weighted normal equations*, which can be written in the matrix form

$$\mathcal{A}^T\Lambda\mathcal{A}\,\mathfrak{Z} = \mathcal{A}^T\Lambda\mathbf{u}_{\mathsf{V}}, \tag{8}$$

by introducing the following definitions. Let us first introduce the N_{V}-sized r.h.s. data vector $\mathbf{u}_{\mathsf{V}}$ and the diagonal N_{V}-order weight matrix Λ,

$$\mathbf{u}_{\mathsf{V}} = \begin{bmatrix} u_1 \\ \vdots \\ u_{N_{\mathsf{V}}} \end{bmatrix}, \qquad \Lambda = \begin{bmatrix} \lambda_1 & & \\ & \ddots & \\ & & \lambda_{N_{\mathsf{V}}} \end{bmatrix}.$$

and the N_{V}-sized auxiliary vectors

$$\mathbf{1} = \begin{bmatrix} 1 \\ \vdots \\ 1 \end{bmatrix}, \quad \delta\mathbf{x} = \begin{bmatrix} x_1 - x_{\mathsf{V}} \\ \vdots \\ x_{N_{\mathsf{V}}} - x_{\mathsf{V}} \end{bmatrix}, \quad \delta\mathbf{y} = \begin{bmatrix} y_1 - y_{\mathsf{V}} \\ \vdots \\ y_{N_{\mathsf{V}}} - y_{\mathsf{V}} \end{bmatrix}.$$

Finally, we introduce the $N_{\mathsf{V}} \times 3$ rectangular matrix $\mathcal{A} = [\mathbf{1},\,\delta\mathbf{x},\,\delta\mathbf{y}]$.

The matrix $\mathcal{A}^T\Lambda\mathcal{A}$ is non-singular for every internal vertex v. Let us observe that, independently of the dimensionality of the vertex v, $\mathcal{A}$ is a maximum rank matrix. Indeed, in σ_{V} there must be at least two cells in the 2-D case whose centroids are non collinear with v. A standard result from matrix theory states that

$$rank(\mathcal{A}^T\Lambda\mathcal{A}) = rank(\mathcal{A}),$$

implying that the matrix $\mathcal{A}^T \Lambda \mathcal{A}$ is non-singular.

Solving (8) we obtain the Least Squares coefficients $\{\omega_k^{\mathsf{v}},\ k \in \sigma_{\mathsf{v}}\}$. These ones coincide with the entries of the first row of the Λ-weighted Moore-Penrose pseudo-inverse of $\mathcal{A}$, and are formally given by

$$\omega_k^{\mathsf{v}} = (1,0,0)(\mathcal{A}^T \Lambda \mathcal{A})^{-1} \mathcal{A}^T \Lambda \mathbf{e}_k, \tag{9}$$

$\mathbf{e}_k$ being the k-th vector of the canonical base of $\mathbb{R}^{N_{\mathsf{v}}}$. Finally, equation (7) follows in view of (9) and by taking $\tilde{u}_{\mathsf{v}} = 0$.

3.2 Boundary Vertex Least Squares Algorithm

As for the internal vertex case, we build the linear approximation (6) of the data set $\{(\mathbf{x}_k,\ u_k),\ k \in \sigma_{\mathsf{v}}\}$ in the Least Squares sense .

As v is a boundary vertex, we introduce the boundary condition of (1) as linear constraints of the form

$$\alpha\, a + \beta \mathbf{b} \cdot \mathbf{n}_{\mathsf{v}} = g(\mathbf{x}_{\mathsf{v}}),$$

where $\mathbf{n}_{\mathsf{v}} = \mathbf{n}(\mathbf{x}_{\mathsf{v}})$, and $g_{\mathsf{v}} = g(\mathbf{x}_{\mathsf{v}})$.

Actually, it turns out to be convenient to distinguish between the two situations at the boundary vertex $\mathsf{v} \in \partial\Omega$:

(i) the domain boundary $\partial\Omega$ is locally regular — at least differentiable — at v;
(ii) the domain boundary $\partial\Omega$ is only Lipschitz continuous at v, i.e. it is a corner.

When the boundary shows at least $\mathcal{C}^1$ regularity at the vertex point $\mathbf{x}_{\mathsf{v}} \in \partial\Omega$, the normal vector $\mathbf{n}_{\mathsf{v}} = \mathbf{n}(\mathbf{x}_{\mathsf{v}})$ can be uniquely defined. In such a case, we minimize the constrained functional

$$\mathcal{J}\,(a, \mathbf{b}, \mu) = \sum_{k \in \sigma_{\mathsf{v}}} \lambda_k \left[a + \mathbf{b} \cdot (\mathbf{x} - \mathbf{x}_{\mathsf{v}}) - u_k\right]^2 + \mu\, (\alpha\, a + \beta \mathbf{b} \cdot \mathbf{n}_{\mathsf{v}} - g_{\mathsf{v}}\,),$$

where μ is a Lagrangian multiplier. Otherwise, we must cope with two distinct normal vectors $\mathbf{n}_{\mathsf{v}}^{(1)}$ and $\mathbf{n}_{\mathsf{v}}^{(2)}$, one for each boundary edge incident v. We take into account this situation by introducing two different lagrangian multipliers μ_1 and μ_2, and by minimizing the constrained functional

$$\mathcal{J}\,(a, \mathbf{b}, \mu) = \sum_{k \in \sigma_{\mathsf{v}}} \lambda_k \left[a + \mathbf{b} \cdot (\mathbf{x} - \mathbf{x}_{\mathsf{v}}) - u_k\right]^2 + \sum_{k=1,2} \mu_k\, (\alpha\, a + \beta \mathbf{b} \cdot \mathbf{n}_{\mathsf{v}}^{(k)} - g_{\mathsf{v}}\,).$$

By repeating the Least Squares procedure, we obtain the augmented system

$$\begin{bmatrix} \mathcal{A}^T\Lambda\mathcal{A} & \mathcal{B} \\ \mathcal{B}^T & 0 \end{bmatrix} \begin{bmatrix} \mathfrak{z} \\ \boldsymbol{\mu} \end{bmatrix} = \begin{bmatrix} \mathcal{A}^T\Lambda\mathbf{u}_{\mathsf{V}} \\ g_{\mathsf{V}} \end{bmatrix}, \tag{10}$$

where $\mathcal{A}$ and $\mathfrak{z}^T = (a,\, \mathbf{b}^T)$ are the 3×3 matrix and the 3-entry vector of unknowns defined in the previous section. The lagrangian multiplier unknown vector $\boldsymbol{\mu}$ and the constraint matrix $\mathcal{B}$ are defined in cases (i) and (ii) by

$$\text{case } (i) \qquad \boldsymbol{\mu} = \begin{bmatrix} \mu \end{bmatrix}, \qquad \mathcal{B} = \begin{bmatrix} \alpha \\ \beta\mathbf{n}_{\mathsf{V}} \end{bmatrix};$$

$$\text{case } (ii) \qquad \boldsymbol{\mu} = \begin{bmatrix} \mu_1 \\ \mu_2 \end{bmatrix}, \qquad \mathcal{B} = \begin{bmatrix} \alpha & \alpha \\ \beta\mathbf{n}_{\mathsf{V}}^{(1)} & \beta\mathbf{n}_{\mathsf{V}}^{(2)} \end{bmatrix}.$$

The augmented system (10) is formally solved by the null space method, which generalises the treatment of internal vertices described in section 3.1 to the boundary vertices. Let us first introduce the kernel matrix of $\mathcal{B}^T$, that is the matrix $\mathcal{K}$ whose columns form by definition a basis for the null-space of $\mathcal{B}^T$. This fact is expressed by the relation $\mathcal{B}^T\mathcal{K} = 0$. Let us then denote by $\hat{\mathfrak{z}} = (\hat{a}, \hat{\mathbf{b}})^T$ a special solution vector such that $\mathcal{B}^T\hat{\mathfrak{z}} = g_{\mathsf{V}}$. Substituting the general solution expression $\mathfrak{z} = \hat{\mathfrak{z}} + \mathcal{K}\boldsymbol{\rho}$ into (10) and projecting onto the null-space of $\mathcal{B}^T$, we obtain the reduced algebraic system

$$\mathcal{K}^T\mathcal{A}^T\Lambda\mathcal{A}\mathcal{K}\boldsymbol{\rho} = \mathcal{K}^T(\mathcal{A}^T\Lambda\mathbf{u}_{\mathsf{V}} - \mathcal{A}^T\Lambda\mathcal{A}\hat{\mathfrak{z}})$$

for the unknown vector $\boldsymbol{\rho}$. Consequently, the solution $\boldsymbol{\rho}$ can be formally written as

$$\boldsymbol{\rho} = (\mathcal{K}^T\mathcal{A}^T\Lambda\mathcal{A}\mathcal{K})^{-1}\mathcal{K}^T\mathcal{A}^T\Lambda(\mathbf{u}_{\mathsf{V}} - \mathcal{A}\hat{\mathfrak{z}}),$$

if we assume that the projected matrix $\mathcal{K}^T\mathcal{A}^T\Lambda\mathcal{A}\mathcal{K}$ is non-singular. This latter issue will be discussed in section 3.3.

A special solution $\hat{\mathfrak{z}}$ can be built in a very simple way by setting $\hat{a} = 0$ and choosing the coefficients of the vector $\hat{\mathbf{b}}$ that satisfy the equation $\hat{\mathbf{b}}\cdot\mathbf{n}_{\mathsf{V}} = g_{\mathsf{V}}$, for instance $\hat{\mathbf{b}} = g_{\mathsf{V}}\mathbf{n}_{\mathsf{V}}$. Notice that this is clearly always possible because $\mathbf{n}_{\mathsf{V}} \neq \mathbf{0}$. Finally, since the linear Least Squares reconstructed value at the vertex v is

$$u_{\mathsf{V}}(\mathbf{x}_{\mathsf{V}}) = a = (1,0,0)\cdot\mathfrak{z} = (1,0,0)\cdot(\hat{\mathfrak{z}} + \mathcal{K}\boldsymbol{\rho}),$$

formula (7) is obtained by defining in case (i)

$$\omega_k^{\mathsf{V}} = (1,0,0)\mathcal{K}(\mathcal{K}^T\mathcal{A}^T\Lambda\mathcal{A}\mathcal{K})^{-1}\mathcal{K}^T\mathcal{A}^T\Lambda\mathbf{e}_k, \tag{11}$$

and

$$\tilde{u}_{\mathsf{V}} = (1,0,0)\left[I - \mathcal{K}(\mathcal{K}^T\mathcal{A}^T\Lambda\mathcal{A}\mathcal{K})^{-1}\mathcal{K}^T\right]\mathcal{A}^T\Lambda\mathcal{A}\,\hat{\mathfrak{Z}}. \tag{12}$$

In case (ii), the weight formula (11) still holds, but (12) defines a two-entry vector $\tilde{\mathbf{u}}_{\mathsf{V}} = (\tilde{u}_{\mathsf{V}}^{(1)},\, \tilde{u}_{\mathsf{V}}^{(2)})^T$, because we have one Least Squares displacement for each contraint. In such case, the Least Squares displacement in (7) is the sum of these latters, i.e. $\tilde{u}_{\mathsf{V}} = \tilde{u}_{\mathsf{V}}^{(1)} + \tilde{u}_{\mathsf{V}}^{(2)}$.

3.3 Existence and uniqueness of the LS reconstructed solution

As $\mathcal{B}^T$ is a maximum rank matrix in both cases (i) and (ii), the projected matrix $\mathcal{K}^T\mathcal{A}^T\Lambda\mathcal{A}\mathcal{K}$ is non-singular if and only if there holds that

$$\textsc{Ker}(\mathcal{B}^T) \cap \textsc{Ker}(\Lambda^{\frac{1}{2}}\mathcal{A}) = \{\mathbf{0}\}. \tag{13}$$

This condition is surely verified because Assumption 2 implies that $\mathcal{A}$ is also a maximum-rank matrix. As anticipated in the previous section, Assumption 2 can be relaxed by admitting the case of a "pathological" boundary vertex belonging to one or two triangles. A unique solution to (10) can still be guaranteed to exist by requiring that (13) be directly satisfied. This leads to ask explicitly for a constraint of the form

$$\Lambda^{\frac{1}{2}}\mathcal{A}\mathcal{K} \neq 0,$$

that must be checked for every pathological vertex and is clearly dependent on the boundary condition coefficients α and β.

3.4 Numerical Stability

As pointed out in References [13,6], the algebraic problem resulting from the weighted normal equations (8) may be ill-conditioned when the mesh is highly stretched. As the sensitivity of the solution of (8) and (10) depends on the square of the condition number of $\mathcal{A}$, the accuracy of the Least Squares weights may be significantly reduced. This situation takes place when the centroids are nearly collinear, that is, when a situation of numerical rank deficiency occurs in the Least Squares resolution process.

In References [13,6] the authors utilizes the weights giving the arithmetics average, i.e. $\boldsymbol{\lambda} = \frac{1}{N_{\mathsf{V}}}\mathbf{I}$, and suggest to apply an orthogonal decomposition in the form $\mathcal{A} = \mathbf{QR}$, $\mathbf{Q}$ denoting as usual the orthogonal matrix and $\mathbf{R}$

the upper triangular matrix of the Gram-Schmidt process. The reconstructed solution is then given by

$$\begin{bmatrix} a \\ \mathbf{b} \end{bmatrix} = \mathbf{R}^{-1} Q^T \mathbf{u}_{\mathsf{V}}.$$

This technique is rather standard in the numerical re-solution of Least Squares problems.

A simpler strategy consists in imposing an *angle condition* at the mesh generation level to avoid excessive mesh stretching and collinear (co-planar in 3-D) centroids.

4 A numerical experiment

In this section we illustrate experimentally the accuracy of the proposed method and its capabilities in reconstructing the vertex values.

The source term f is calculated in order to have the following exact solution

$$u^{(ex)}(x, y) = x\, y\, \exp(x + y)$$

on the domain $\Omega = [0,\, 1] \times [0,\, 1]$.

As depicted in Figure 4, boundary conditions of Dirichlet type, i.e. $\alpha = 1$, $\beta = 0$, are imposed to the vertices at $x = 0$ and at $x = 1$. The vertices at the top side of the domain, $y = 1$, are given a Neumann type condition, i.e. $\alpha = 0$, $\beta = 1$, and the ones at the bottom side, $y = 0$, a Robin type condition, $\alpha = \beta = 1$. The lower-left vertex is given a Neumann type condition, the upper-right one a Robin type condition, and the other two corner vertices a Dirichlet type condition.

All of the calculations are performed on a set of four unstructured grids built as follows. The base grid is formed by 162 triangles and has been generated by using the public domain software Triangle; the grids at the next refinement levels are obtained by a nested subdivision process. That is, each triangle at a given refinement level is subdivided into four triangles by connecting its edge mid-points. Notice that this partitioning strategy preserves the shape, that is the aspect ratio, of the triangular mesh cells.

The steady solutions for the first three mesh calculations are shown in Figure 2, whild Table 1 summarizes the results of all of the four simulation runs. The first three columns respectively report the number of the mesh cells, $\#T$, the

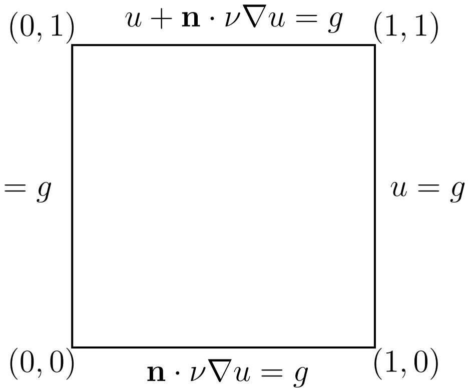
$(0,1)$
$u + \mathbf{n} \cdot \nu \nabla u = g$
$(1,1)$
$u = g$
$u = g$
$(0,0)$
$\mathbf{n} \cdot \nu \nabla u = g$
$(1,0)$

Fig. 1. Boundary conditions

number of mesh edges, $\#E$, and the number of boundary edges, $\#BE$. The forth column reports the relative error $\mathcal{E}^{rel}$ of the cell-averaged concentration with respect to the analytical solution. This error is measured by using a discrete version of the L^2 norm; that is

$$\mathcal{E}^{rel} = \frac{\sqrt{\sum_{\mathsf{T}_i \in \mathcal{T}_h} |\mathsf{T}_i| \, \left|u_i - u^{(ex)}(\mathbf{x}_i)\right|^2}}{\sqrt{\sum_{\mathsf{T}_i \in \mathcal{T}_h} |\mathsf{T}_i| \, \left|u^{(ex)}(\mathbf{x}_i)\right|^2}}. \tag{14}$$

The fifth column gives the rate of convergence rate measured when the mesh factor h is halved in the mesh refinement process. These numbers indicates the order of accuracy in the approximation of a suitably smooth solution, and are calculated by applying the formula

$$\mathsf{Rate}(h, h/2) = \log_2 \frac{\mathcal{E}^{rel}_h}{\mathcal{E}^{rel}_{h/2}},$$

to the relative errors $\mathcal{E}^{rel}_h$ and $\mathcal{E}^{rel}_{h/2}$ of two successive lines in the tables.

The next three columns repeat the same information about the linearly-reconstructed vertex concentration. The errors are calculated by a formula similar to (14), that is

$$\widetilde{\mathcal{E}}^{rel} = \frac{\sqrt{\sum_{\mathsf{v} \in \mathcal{V}^h_\Omega} |\mathsf{v}| \, \left|u_{\mathsf{V}} - u^{(ex)}(\mathbf{x}_{\mathsf{V}})\right|^2}}{\sqrt{\sum_{\mathsf{v} \in \mathcal{V}^h_\Omega} |\mathsf{v}| \, \left|u^{(ex)}(\mathbf{x}_{\mathsf{V}})\right|^2}},$$

where $\mathcal{V}^h_\Omega$ is the set of all of the vertices of the mesh, $|\mathsf{v}| = \sum_{\mathsf{V} \in \sigma_{\mathsf{V}}} |\mathsf{T}_{\mathsf{V}}|$ is the cumulative area of the triangles surrounding the vertex v, and σ_{V} the set of indices of these latter triangles. The convergence rate of the vertex reconstructed values has the same definition of the convergence for the cell-average values previously introduced. It is evident from the results in Table 1 that second-order convergence is attained in nearly all of the runs, thus confirming the theoretical convergence rate. The corsest grids show the worst resolution

Table 1
Absolute and relative errors and convergence rates for $\nu = 1$.

$\#lev$	$\#T$	$\#E$	$\#BE$	$\mathcal{E}^{rel}$	Rate	$\widetilde{\mathcal{E}}^{rel}$	Rate
1	162	259	32	$6.11\,10^{-3}$	—	$1.12\,10^{-3}$	—
2	648	1004	64	$1.46\,10^{-3}$	2.06	$3.35\,10^{-3}$	1.88
3	2592	3952	128	$3.56\,10^{-4}$	2.03	$8.68\,10^{-4}$	1.94
4	10368	15680	256	$8.77\,10^{-5}$	2.02	$2.21\,10^{-4}$	1.97

as one can expect, and consequently the worst accuracy in the spatial approximation. Nevertheless, by increasing the mesh resolution, the spatial accuracy increases and tends towards the order $\mathcal{O}(h^2)$, as predicted by the theory.

5 Conclusions

We introduced the theoretical framework of an alternative approach to the usual ghost cell method for the treatment of boundary conditions in Least Squares-based cell-centered finite volume discretisations of two-dimensional second-order steady diffusion problems.

The Least Squares vertex reconstruction can be re-formulated in a unified way to take into account both internal and boundary vertices. In the former case, we apply the standard Least Squares reconstruction process which is solved by the normal equation technique. In the latter case, a constrained Least Squares process is considered that takes into account at the vertex reconstruction level Dirichlet, Neumann and Robin conditions for the boundary vertices.

The method has been discussed in full details, and its application to a representative numerical test case demonstrated its compatibility to second-order accurate Least Squares-based cell-centered Finite Volumes.

References

[1] C. Hirsch, Numerical Computation of Internal and External Flows, J. Wiley & Sons Ltd., Baffins Lane, Chichester, West Sussex PO19 1UD, England, 1990.

[2] A. Quarteroni, A. Valli, Numerical approximation of partial differential equations, Springer-Verlag, Berlin, 1994.

[3] Y. Coudière, J.-P. Vila, P. Villedieu, Convergence rate of a finite volume scheme for a two dimensional convection-diffusion problem, M2AN. Mathematical Modelling and Numerical Analysis 33 (3) (1999) 493–516.

[4] Y. Coudière, P. Villedieu, Convergence rate of a finite volume scheme for the linear convection-diffusion equation on locally refined meshes, M2AN Math. Model. Numer. Anal. 34 (6) (2000) 1123–1149.

[5] E. Bertolazzi, G. Manzini, Contaminant transport in porous media by a finite volume method, Applied Numerical Mathematics.

[6] W. K. Anderson, D. L. Bonhaus, An implicit upwind algorithm for computing turbulent flows on unstructured grids, Computers Fluids 23 (1) (1994) 1–21.

[7] N. T. Frink, P. Parikh, S. Pirzadeh, A fast upwind solver for the euler equations on three-dimensional unstructured meshes, in: Computational Fluid Dynamic Conference, no. AIAA-91-0102, AIAA, 1991, pp. 1–6.

[8] N. T. Frink, Recent progress toward a three-dimensional unstructured navier-stokes solver, in: 32^{th} Aerospace Sciences Meeting, no. AIAA-94-0061, AIAA, 1994, pp. 1–20.

[9] N. T. Frink, S. Pirzadeh, Tetrahedral finite-volume solutions to the navier-stokes equations on complex configurations, Tech. Rep. AIAA-98-208961 (1998).

[10] E. Bertolazzi, G. Manzini, Limiting strategies for polynomial reconstructions in Finite Volume approximations of the linear advection equation, in: SIMAI, 2002.

[11] R. Eymard, T. Gallouët, R. Herbin, Finite volume methods, in: Handbook of numerical analysis, Vol. VII, North-Holland, Amsterdam, 2000, pp. 713–1020.

[12] P. G. Ciarlet, The finite element method for elliptic problems, North-Holland Publishing Company, Amsterdam, Holland, 1980.

[13] T. J. Barth, D. C. Jespersen, The design and applications of upwind schemes on unstructured meshes, in: 27^{th} Aerospace Sciences Meeting, no. AIAA-89-0366, AIAA, 1989, pp. 1–12.

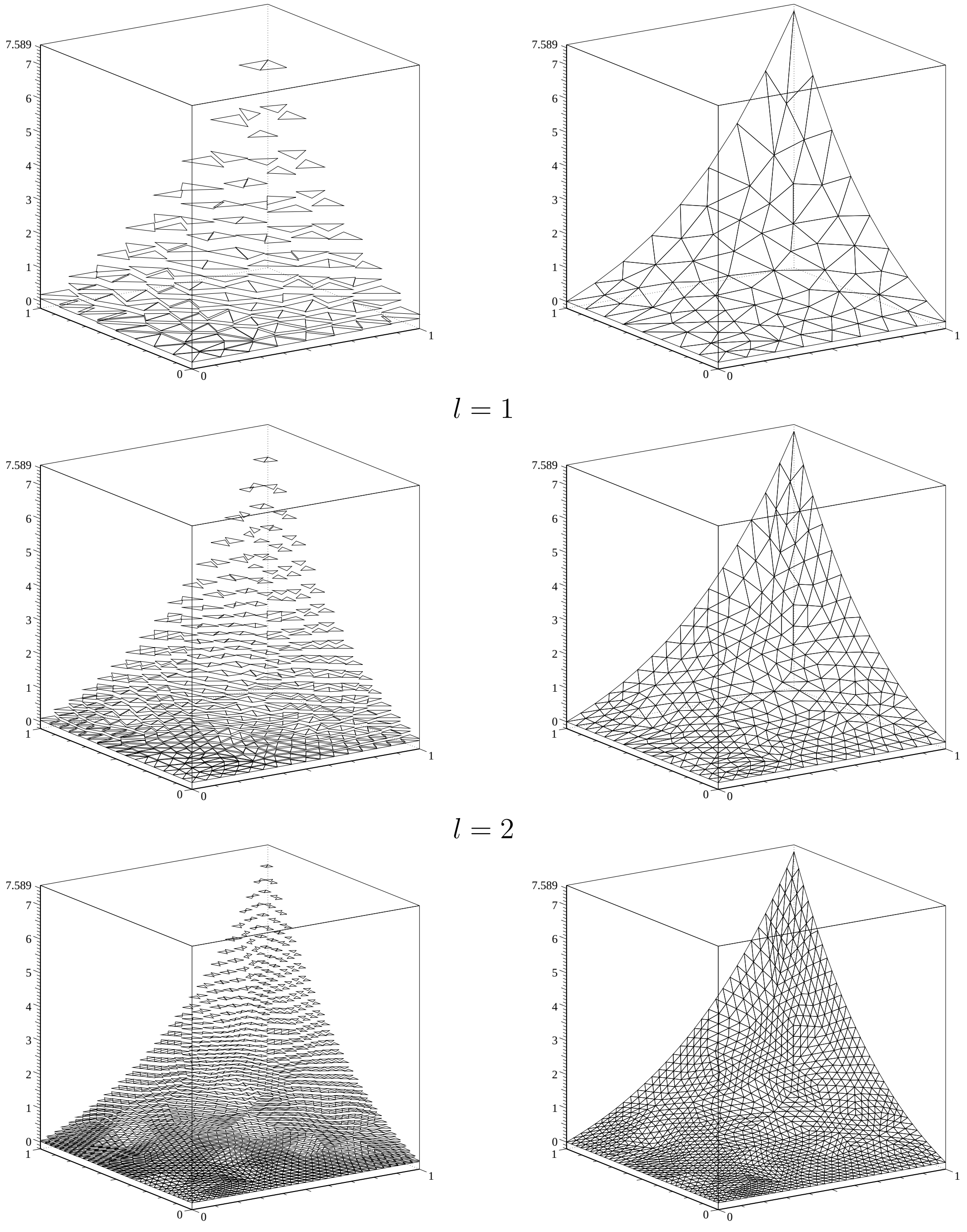

$l = 1$

$l = 2$

$l = 3$

Fig. 2. Steady diffusion equation on three different refinement level meshes, $l = 1$, 2, 3; cell-averaged solutions are displayed on the left and linearly-reconstructed vertex solutions on the right.